


FULL ARTICLE

# Characterizing near-infrared spectroscopy signal under hypercapnia

Ho-Ching (Shawn) Yang<sup>1</sup>  | Zhenhu Liang<sup>1,2</sup> | Nicole L. Vike<sup>3</sup> | Taylor Lee<sup>4</sup> | Joseph V. Rispoli<sup>1,5</sup> | Eric A. Nauman<sup>1,4</sup> | Thomas M. Talavage<sup>1,5</sup> | Yunjie Tong<sup>1\*</sup>

<sup>1</sup>Weldon School of Biomedical Engineering, Purdue University, West Lafayette, Indiana

<sup>2</sup>Institute of Electrical Engineering, Yanshan University, Qinhuangdao, China

<sup>3</sup>Department of Basic Medical Sciences, Purdue University, West Lafayette, Indiana

<sup>4</sup>School of Mechanical Engineering, Purdue University, West Lafayette, Indiana

<sup>5</sup>School of Electrical and Computer Engineering, Purdue University, West Lafayette, Indiana

## \*Correspondence

Yunjie Tong, Weldon School of Biomedical Engineering, Purdue University, West Lafayette, IN 47907, USA.

Email: tong61@purdue.edu

## Funding information

National Science Foundation, Grant/Award Number: Graduate Research Fellowship (NSF GRFP DGE-1333468); Indiana Clinical and Translational Sciences Institute, Grant/Award Number: the Pilot Funding for Research Use of Core Facility; National Institutes of Health, Grant/Award Number: K25 DA031769 (YT)

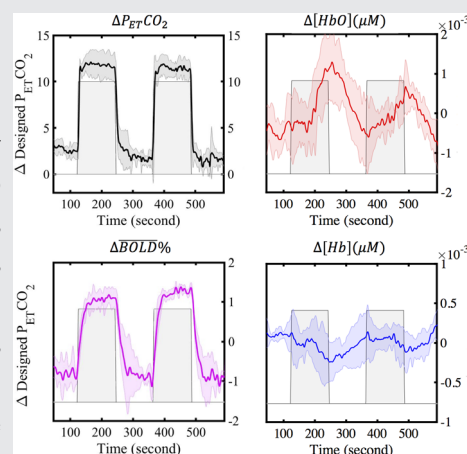
## Abstract

Vasoactive stress tests (i.e. hypercapnia, elevated partial pressure of arterial CO<sub>2</sub> [PaCO<sub>2</sub>]) are commonly used in functional MRI (fMRI), to induce cerebral blood flow changes and expose hidden perfusion deficits in the brain. Compared with fMRI, near-infrared spectroscopy (NIRS) is an alternative low-cost, real-time, and non-invasive tool, which can be applied in out-of-hospital settings. To

develop and optimize vasoactive stress tests for NIRS, several hypercapnia-induced tasks were tested using concurrent-NIRS/fMRI on healthy subjects. The results indicated that the cerebral and extracerebral reactivity to elevated PaCO<sub>2</sub> depended on the rate of the CO<sub>2</sub> increase. A steep increase resulted in different cerebral and extracerebral reactivities, leading to unpredictable NIRS measurements compared with fMRI. However, a ramped increase, induced by ramped-CO<sub>2</sub> inhalation or breath-holding tasks, induced synchronized cerebral, and extracerebral reactivities, resulting in consistent NIRS and fMRI measurements. These results demonstrate that only tasks that increase PaCO<sub>2</sub> gradually can produce reliable NIRS results.

## KEYWORDS

cerebral blood flow, hypercapnia, magnetic resonance imaging, near-infrared spectroscopy



## 1 | INTRODUCTION

Vasoactive stress tests (i.e. hypercapnia, elevated partial pressure of arterial CO<sub>2</sub> [PaCO<sub>2</sub>]) are widely used in imaging studies to expose hidden brain perfusion deficits by increasing cerebral blood flow (CBF).<sup>1–3</sup> Hypercapnia, a condition where CO<sub>2</sub> is elevated, is known to cause a global increase in CBF due to the potent effect of CO<sub>2</sub> as

a vasodilator.<sup>4</sup> Increasing PaCO<sub>2</sub> decreases pH and relaxes vascular smooth muscle cells in arteries, ultimately leading to an increase in CBF.<sup>5, 6</sup> The end-tidal CO<sub>2</sub> (P<sub>ET</sub>CO<sub>2</sub>; the concentration of CO<sub>2</sub> at the end of exhaled breath) is commonly used as surrogate signal for PaCO<sub>2</sub>.<sup>1–3, 7, 8</sup>

There are two common methods used to induce hypercapnia. The first method is CO<sub>2</sub> inhalation, which requires a subject to wear a breathing mask that is

connected to a system, which controls the mixture and flow rates of gases (e.g. O<sub>2</sub>, N<sub>2</sub>, and CO<sub>2</sub>).<sup>9, 10</sup> This method can either deliver a fixed concentration of CO<sub>2</sub> or target a subject-specific P<sub>ET</sub>CO<sub>2</sub> level for a period of time (~120 seconds).<sup>2, 11–13</sup> Because this method allows subjects to inhale CO<sub>2</sub> passively, it is called CO<sub>2</sub> inhalation, or CI. Second, the breath-holding (BH) task requires subjects to hold their breath for short periods of time (~20 seconds). This method also results in an increase of P<sub>ET</sub>CO<sub>2</sub> and a subsequent increase in CBF.<sup>14, 15</sup> The BH task is a simpler means to induce hypercapnia compared with the CI task since it does not require additional specialized equipment.

Near-infrared spectroscopy (NIRS) is a noninvasive optical device that has been widely used to investigate concentrations of oxyhemoglobin ( $\Delta$ [HbO]) and deoxyhemoglobin ( $\Delta$ [Hb]) at the surface of the cortex, thereby providing measurements of cerebral blood flow (CBF), volume, and oxygenation changes.<sup>16–19</sup> Compared with functional magnetic resonance imaging (fMRI), NIRS is a low-cost, portable technology for studying brain function and physiology.<sup>18</sup> Recently, some studies have used NIRS to study hypercapnia under the CI and BH tasks.<sup>20–26</sup> There are several benefits of using NIRS in vasoactive stress tests. For example, NIRS can provide real-time cerebral vascular reactivity (CVR) measurements on the football field, as chronic brain damage has prompted concern for contact sport athletes.<sup>27–29</sup> Also, NIRS can provide bedside CVR measurements for immobile elderly people.<sup>30, 31</sup> However, results from CI tasks have been inconsistent; this may be due to physiological noise coming from skin and skull.<sup>32–34</sup> For example, two studies reported that NIRS signals correlated well with P<sub>ET</sub>CO<sub>2</sub> under the CI task,<sup>20, 25</sup> but other studies found that NIRS signals were not sensitive to P<sub>ET</sub>CO<sub>2</sub> under the CI task.<sup>22–24</sup> The goals of this study were to better understand NIRS signals during different hypercapnia tasks and develop a robust and independent NIRS protocol to assess brain reaction to vasostimulus. The NIRS signals ( $\Delta$ [HbO] and  $\Delta$ [Hb]) and fMRI blood oxygenation level dependent (BOLD) signals were compared for consistency with the goal of validating NIRS as a portable fMRI proxy.

## 2 | MATERIALS AND METHODS

### 2.1 | Protocol

This study was approved by Purdue University Institutional Review Board. Informed consent was obtained from all subjects. 10 healthy subjects (4 female, 6 male, age range 19–33, mean age 23 years) were recruited for

several hypercapnia tasks measured by NIRS and fMRI concurrently (Figure 1A–D).

### 2.2 | Near-infrared spectroscopy

The CW NIRS system (NIRScoutXP NIRx Medizintechnik GmbH; Berlin, Germany) and MRI-compatible NIRS probes with 10 m long optical fibers were used to measure  $\Delta$ [HbO] and  $\Delta$ [Hb]. This system uses laser sources, each combining two wavelengths (785 and 830 nm). The source-detector distance was 3 cm. Vascular reactions to hypercapnia were recorded from the prefrontal region of the brain. Due to the limited space in MRI head coil, 17 NIRS channels (7 sources and 7 detectors) were deployed with a sampling rate of 7.8125 Hz (Figure 1E).

### 2.3 | MRI

Functional MRI data were obtained using a 3 T GE Discovery MR750 MR scanner (GE Electric; Milwaukee, WI) and a 32-channel receiver head coil (Nova Medical, Inc.; Wilmington, MA). The MRI scans were acquired using a multiband echo-planar imaging sequence (FOV = 216 mm, acquisition matrix = 72 × 72, 60 slices, voxel size = 3 × 3 × 3 mm<sup>3</sup>, TR/TE = 1000/30 ms, flip angle = 50°, hyperband acceleration factor = 4, phase acceleration factor = 1).

### 2.4 | Sharp-CO<sub>2</sub> inhalation (sharp-CI) task

For the sharp-CI task, varying CO<sub>2</sub> concentrations were supplied to each subject, through a sealed mask, by a computerized gas delivery system (RespirAct, Thornhill Research Inc. Toronto, Canada; Figure 1F).<sup>9</sup> P<sub>ET</sub>CO<sub>2</sub> and P<sub>ET</sub>O<sub>2</sub> were controlled and measured throughout the experiment. All subjects took part in pre-testing outside the MRI to ensure they were capable and comfortable performing the sharp-CI task. The pre-testing consisted of (a) a measurement of each subject's baseline P<sub>ET</sub>CO<sub>2</sub> and (b) a short version of the sharp-CI task. The full task consisted of five 2-minute blocks (Figure 1A). The 1st, 3rd and 5th blocks were rest blocks where subjects inhaled normal air. The 2nd and 4th blocks were hypercapnia blocks where subjects inhaled air with sharply elevated CO<sub>2</sub> concentration that led to an increase of 10 mmHg above each subject's P<sub>ET</sub>CO<sub>2</sub> baseline within one or two breaths. The P<sub>ET</sub>CO<sub>2</sub> was then maintained at the high level for 2 minutes (Figure 1A).<sup>35</sup>

**FIGURE 1** Experimental design and setup. Schematic of A, the sharp-CI, B, the long-ramped CI, C, the BH, and D, the short-ramped CI tasks. E, Configuration of the NIRS channels on the head. F, Experimental setup of the concurrent fMRI/NIRS experiments

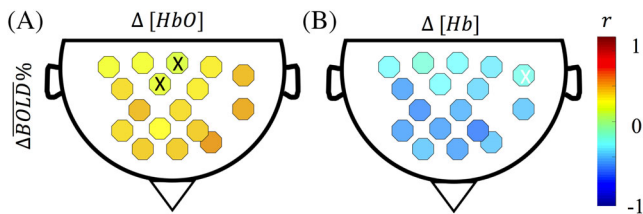
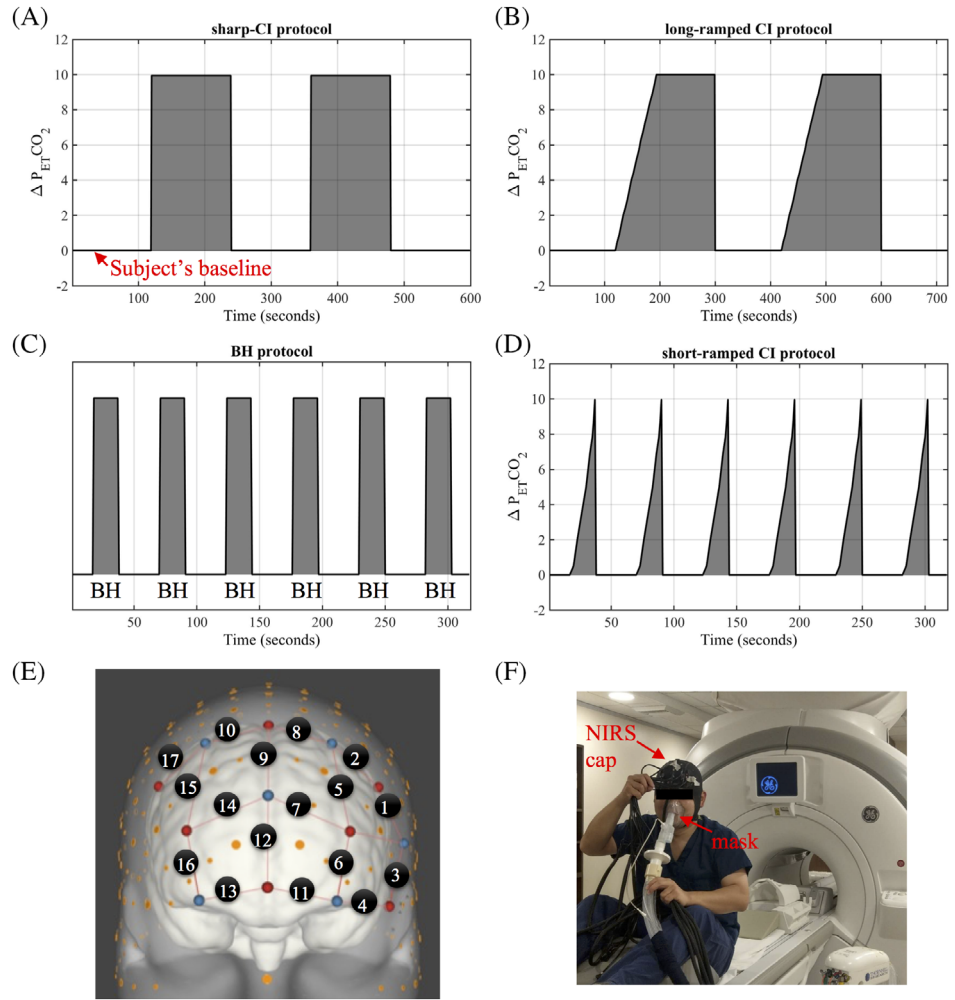


**FIGURE 2** Averaged maximum cross-correlation coefficient from each channel under the sharp-CI task between percent change of averaged BOLD signal ( $\Delta BOLD\%$ ) and A,  $\Delta[HbO]$  and B,  $\Delta[Hb]$ . Crosses in the channel indicate a  $p$ -value larger than 0.05 under the FDR-criterion

## 2.5 | Other induced-hypercapnia tasks

To further explain inconsistencies between the NIRS and fMRI signals under the sharp-CI task (Figures 2 and 3), we conducted three additional concurrent-fMRI/NIRS experiments on 4 out of the original 10 subjects (2 male, 2 female, age range 20-29, mean age 22 years, subgroup). These additional experiments (i.e., long-ramped CI, BH, and short-ramped CI tasks) examined the effects of the rate of hypercapnia inducement on NIRS and fMRI data.

First, the sharp-CI task was modified to incorporate the long-ramped increase in  $P_{ET}CO_2$ , called long-ramped CI task (as shown in Figure 1B).<sup>25</sup> In short, during the hypercapnia blocks, the  $P_{ET}CO_2$  was slowly ramped up to 10 mmHg above subject's baseline within 75 seconds, and then maintained at that level for 105 seconds.

Second, the BH task was adopted from a widely used paradigm.<sup>36</sup> It consisted of 6 BH epochs (Figure 1C); each epoch had 18 seconds of paced breathing (3 repetitions of a 3 seconds inhale followed by a 3 seconds exhale), followed by 20 seconds of BH, and then 15 seconds of normal breathing (total time = 5 minutes 18 seconds). To acquire consistent results from the BH task across all subjects, a gentle exhale was required prior to the BH.<sup>36</sup> An open source package from PsychoPy was compiled to provide instructions to subjects and control procedures (i.e. paced breathing, BH, and normal breathing).<sup>37</sup>

Finally, a short-ramped  $P_{ET}CO_2$  was designed (Figure 1D) to simulate the BH task via  $P_{ET}CO_2$  control. In short, the short-ramped CI paradigm began with 18 seconds of rest followed by six blocks of alternating hypercapnia sections. The first hypercapnia section slowly ramped the

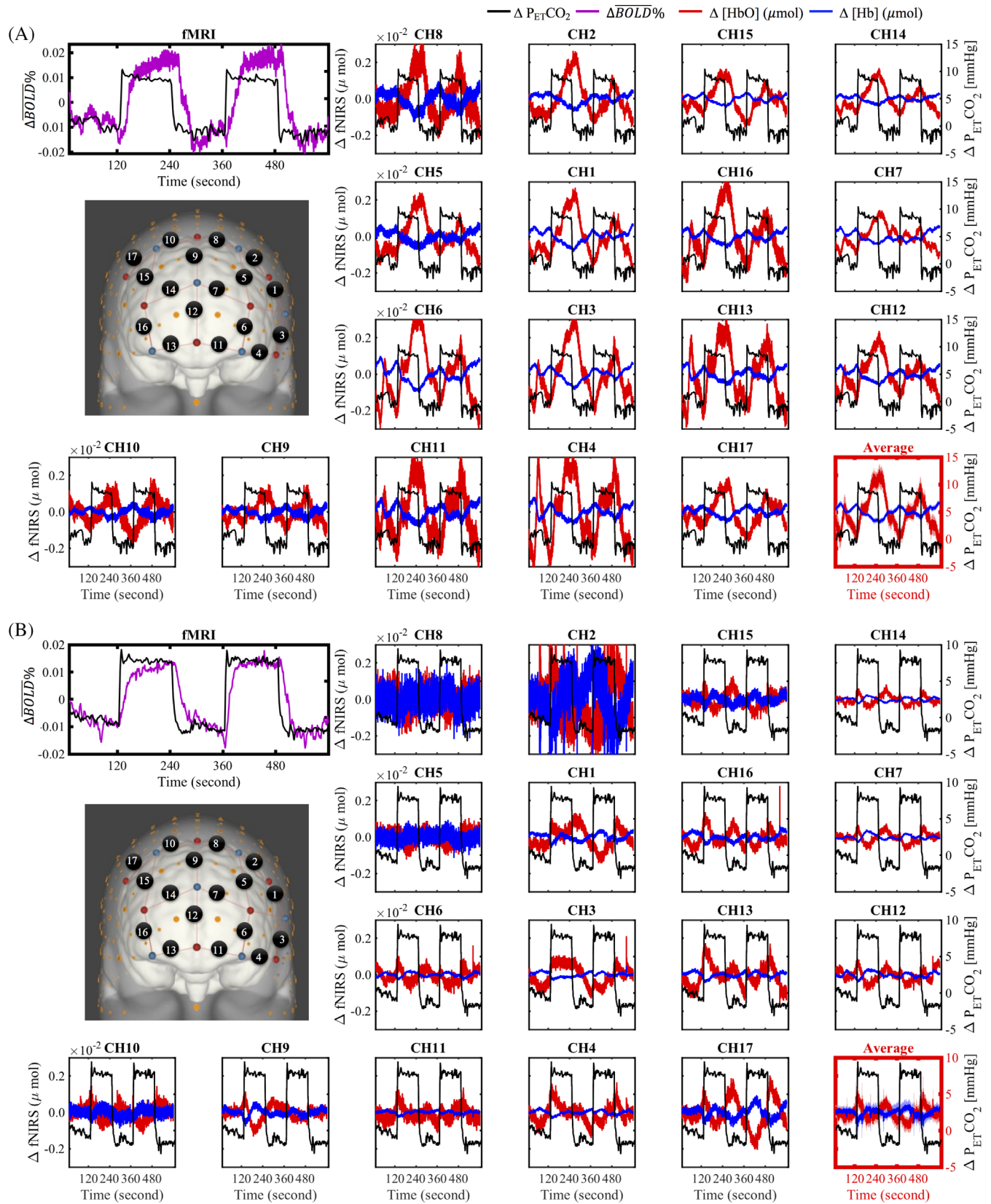


**FIGURE 3** Results showing inconsistencies in NIRS signals during the sharp-CI task from two example subjects in A and B. The signals of  $\Delta P_{ET}CO_2$ ,  $\Delta \overline{BOLD}\%$ ,  $\Delta [HbO]$ , and  $\Delta [Hb]$  are shown in the colors of black, purple, red, and blue, respectively. The averaged results of  $\Delta [HbO]$  and  $\Delta [Hb]$  are shown at bottom right of A and B in red boxes



subject's  $P_{ET}CO_2$  to 10 mmHg above their baseline within 20 seconds, and the second section consisted of normal breathing for 33 seconds. The 10 mmHg increase of  $P_{ET}CO_2$  was selected based on a study by Tancredi et al, which demonstrated that the  $P_{ET}CO_2$  elevation after a 20 seconds BH was close to 10 mmHg.<sup>38</sup>

## 2.6 | Data analysis

All NIRS data were processed using the nirsLAB analysis package (v2016.05, NIRx Medical Technologies, LLC.; Los

Angeles)<sup>39</sup> and MATLAB (MATLAB 2018b, The MathWorks Inc., Natick, MA, 2000). NIRS signals with bad signal quality were eliminated (i.e. signals with no visible heartbeat signal, Figure S1). For the BH and short-ramped CI task, NIRS signals from those 6 cycles were parsed and aligned to calculate the folding-average result.<sup>40</sup>

All MR data were processed using FSL (FMRIB Expert Analysis Tool, v6.01; Oxford University, UK<sup>41</sup>) and MATLAB. The fMRI BOLD signals acquired during the CI and BH tasks were preprocessed with the following steps recommended by Power et al: (a) motion correction (FSL mcflirt) and (b) spatial smoothing with a full

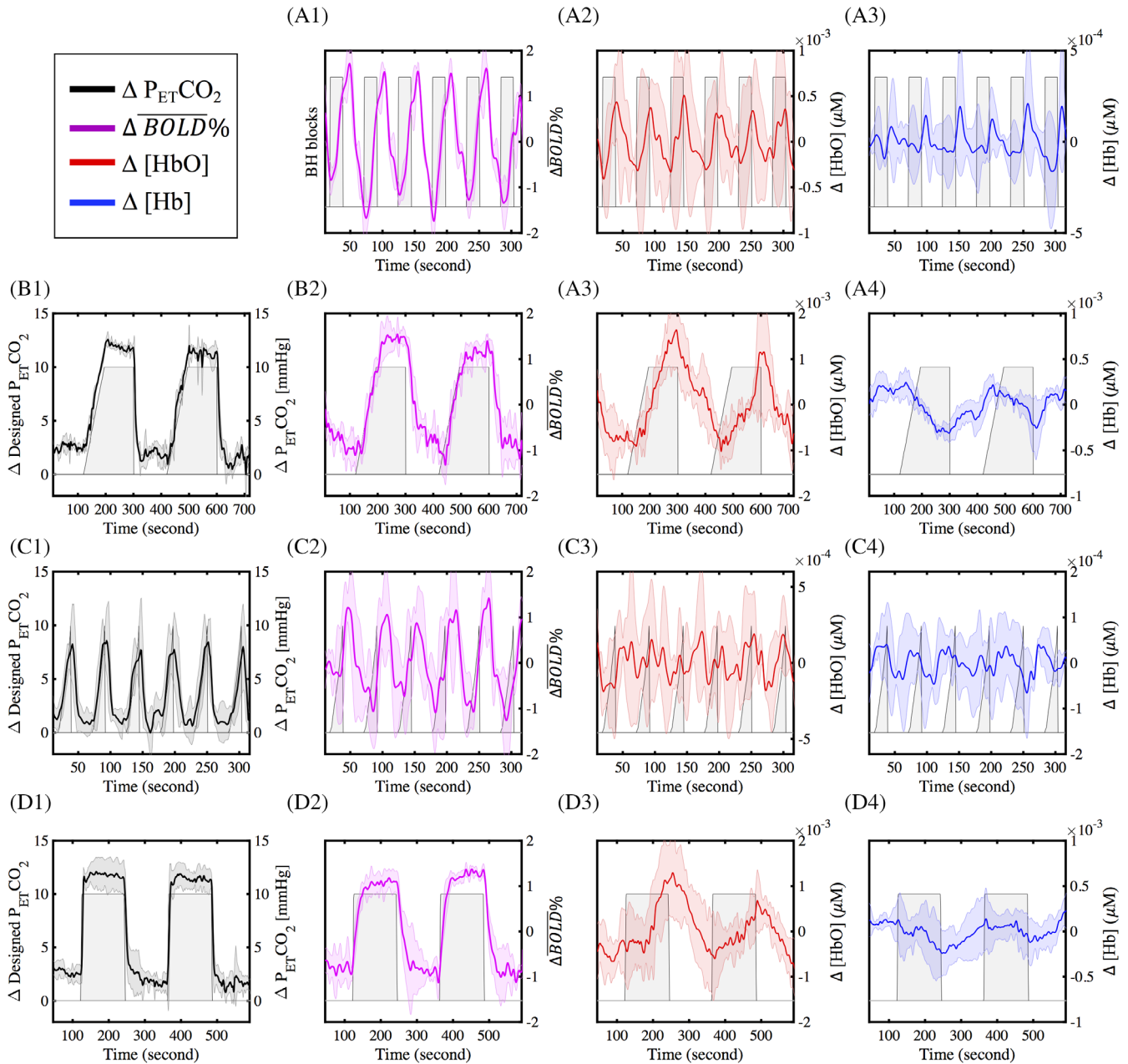


**FIGURE 4** The fMRI and NIRS results from the A, BH, B, long-ramped CI, C, short-ramped CI, and D, sharp-CI tasks. The shaded areas indicate the targeted  $\Delta P_{ET}CO_2$  in each task. The averaged  $\Delta P_{ET}CO_2$ ,  $\Delta BOLD\%$  (normalized),  $\Delta [HbO]$ , and  $\Delta [Hb]$  signals are shown in columns 1–4, respectively

width at half maximum (FWHM) of 5 mm isotropic Gaussian kernel.<sup>42</sup> For comparison with NIRS data, the percent change of averaged BOLD signal ( $\Delta\overline{BOLD}\%$ ) from the prefrontal region was calculated to represent the intracerebral signal in the brain. In short, a prefrontal ROI was created on the standard structural brain and then warped onto each subject's fMRI space to extract the corresponding temporal fMRI signals.<sup>43</sup> Finally, the time series of BOLD signals from all the voxels were averaged (FSL fslmeants) and then normalized (subtracted by mean and divided by SD).

For the sharp-CI and long-ramped CI task, a zero-delay lowpass filter (0.1 Hz, 3th order) was used to extract the low frequency signals ( $\Delta P_{ET}CO_2$ ,  $\Delta\overline{BOLD}\%$ ,  $\Delta[HbO]$ , and  $\Delta[Hb]$ ), since both tasks contain low frequency components ( $<0.005$  Hz). For BH and short-ramped CI tasks, a zero-delay bandpass filter (0.01–0.1 Hz, 3th order) was used to extract the low frequency signals.

To visualize the group result from each experiment, averaged  $\Delta[HbO]$  and  $\Delta[Hb]$  signals from each subject were first subtracted by mean and then averaged by the number of subjects in the group.

To calculate the correlation between signals (NIRS signals,  $\Delta\overline{BOLD}\%$ , and  $\Delta P_{ET}CO_2$ ), cross-correlation (MATLAB xcorr, lag range =  $\pm 45$  seconds) was

performed, knowing time delays might exist among these signals. For statistical analysis, the maximum cross-correlation coefficients (MCCCs) were converted into Z-values using Fisher's Z-transformation (Equation. 1).<sup>44, 45</sup> Then, a one-sample *t* test against zero was applied on the correlation Z-values. The significance level was set at  $p < .05$ , which was corrected for multiple comparisons using the false discovery rate (FDR) criterion.<sup>46</sup> For the additional induced-hypercapnia tasks (4 subjects), the *p*-value was not corrected for multiple comparisons due to the small sample size.

$$Z = \frac{1}{2} \ln \frac{1+r}{1-r} \quad (1)$$

Movies were created to reflect the spatio-temporal changes of NIRS signals,  $\Delta P_{ET}CO_2$ , and especially the regional  $\Delta\overline{BOLD}\%$  under hypercapnia tasks. Tasks included the sharp-CI task (one example with high correlations between  $\Delta\overline{BOLD}\%$ ,  $\Delta P_{ET}CO_2$ , and NIRS signals and another example with low correlations), the BH task, and the long-ramped CI task.

### 3 | RESULTS

#### 3.1 | Sharp-CI results

Consistent  $\Delta\overline{BOLD}\%$  were found across all subjects under the sharp-CI task, which were highly correlated to the waveform of  $\Delta P_{ET}CO_2$  ( $r = 0.89 \pm 0.07$ ,  $p < 10^{-7}$ ). However, inconsistent NIRS signals were found across subjects. For example, averaged NIRS signals had much lower correlation values, and larger standard deviations, when  $P_{ET}CO_2$  was increased sharply ( $\Delta[HbO]$ :  $r = 0.45 \pm 0.44$ ,  $p < 10^{-3}$ ;  $\Delta[Hb]$ :  $r = -0.69 \pm 0.20$ ,  $p < 10^{-4}$ ).

More importantly, averaged NIRS signals showed low correlation with  $\Delta\overline{BOLD}\%$  ( $\Delta[HbO]$ :  $r = 0.43 \pm 0.28$ ,  $p < 10^{-3}$ ;  $\Delta[Hb]$ :  $r = -0.51 \pm 0.32$ ,  $p < 10^{-3}$ ). In fact, correlations between  $\Delta\overline{BOLD}\%$  and NIRS signals were low in most of the channels (Figure 2) and the lowest averaged MCCC between  $\Delta\overline{BOLD}\%$  and  $\Delta[HbO]$  was 0.14. Also, the averaged MCCCs were spatially different. The averaged MCCCs between the  $\Delta P_{ET}CO_2$  and NIRS signals from each channel around the prefrontal region for the original sharp-CI task are mentioned in the supplemental material (Figure S2). To highlight NIRS signal inconsistencies, two subjects are discussed in detail.

The results from the sharp-CI task observed from subject 1 presented good signal correlations between  $\Delta\overline{BOLD}\%$ ,  $\Delta P_{ET}CO_2$ , and NIRS signals (Figure 3A). Under the sharp-CI task,  $\Delta\overline{BOLD}\%$  was highly correlated with  $\Delta P_{ET}CO_2$  ( $r = 0.86$ ; Figure 3A), indicating a fast vascular

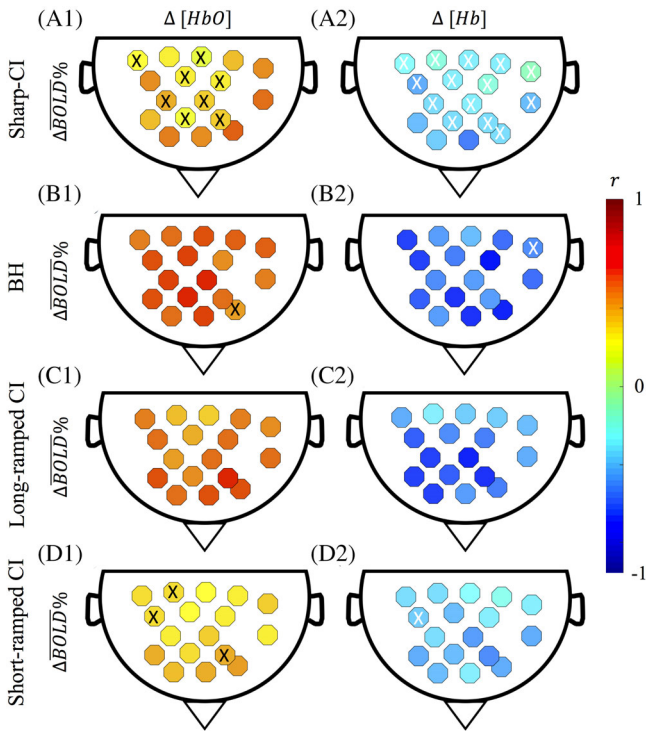


**FIGURE 5** Averaged MCCCs between  $\Delta\overline{BOLD}\%$  and  $\Delta[HbO]$  ( $\Delta[Hb]$ ) signals are shown in column 1 (2). The corresponding tasks are: A, BH; B, long-ramped CI; C, short-ramped CI; D, sharp-CI. Crosses in the channel indicate a *p*-value larger than 0.05 under one-sample *t* test

reaction in the brain. Additionally, although MCCCs between NIRS signals and  $\Delta BOLD\%$  were not low ( $\Delta[HbO]$ :  $r = 0.63 \pm 0.12$ ,  $p < 10^{-9}$ ;  $\Delta[Hb]$ :  $r = -0.57 \pm 0.13$ ,

$p < 10^{-9}$ ), most  $\Delta[HbO]/\Delta[Hb]$  signals responded slowly to the sharp increase of  $P_{ET}CO_2$ . Moreover,  $\Delta[HbO]$  signals (e.g., CH16) continued to increase following

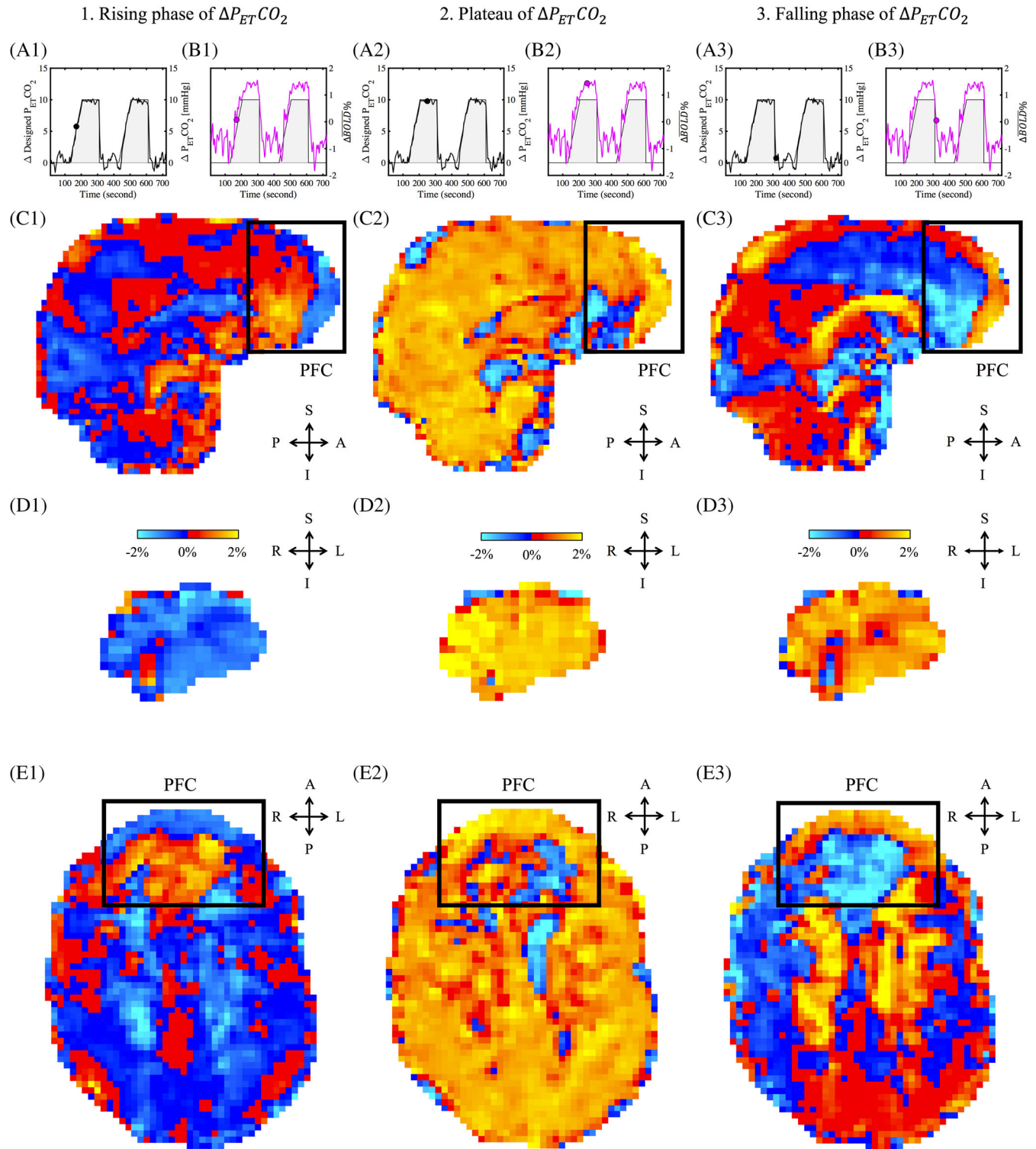


**FIGURE 6** The fMRI movie snapshots from one subject under the long-ramped CI task. Three snapshots were captured at (1) rising phase (2) plateau, and (3) falling phase of  $\Delta P_{ET}CO_2$  in the long-ramped CI task. During each time point, real-time A,  $\Delta P_{ET}CO_2$  and B,  $\Delta BOLD\%$  signals are displayed. Also,  $\Delta BOLD\%$  maps (red-yellow refers to positive percent changes and blue-light blue refers to negative percent changes) in C, sagittal, D, coronal, and E, axial views are shown. The shaded areas indicate the targeted  $\Delta P_{ET}CO_2$  during the task. The black square in every (c) and (e) panel indicate the region of prefrontal cortex (PFC)



cessation of the hypercapnic block and it took a full 2 minutes to decrease during the resting block.

In another subject (e.g., subject 2), NIRS signals did not correlate well with  $\Delta\overline{BOLD}\%$  (Figure 3B,  $\Delta[\text{HbO}]: r = 0.08 \pm 0.20, p > .05$ ;  $\Delta[\text{Hb}]: Z = -0.08 \pm 0.17, p > .05$ ), and did not appear to react to the sharp-increase in  $P_{\text{ETCO}_2}$ . Further, the  $\Delta[\text{HbO}]$  signals, which showed good signal quality and consistency among channels, hardly changed during the first hypercapnic block, but instead increased during the resting block. Interestingly,  $\Delta\overline{BOLD}\%$  for this subject increased sharply with a sharp increase in  $P_{\text{ETCO}_2}$  ( $Z = 0.94$ ), as seen with subject 1 (Figure 3A).

### 3.2 | Additional induced-hypercapnia tasks

The  $\Delta P_{\text{ETCO}_2}$ ,  $\Delta\overline{BOLD}\%$ , and NIRS signals under the BH task, long-ramped CI, short-ramped CI, and sharp-CI task from four selected subjects were also averaged (Figure 4). In all tasks,  $\Delta\overline{BOLD}\%$  signals were highly correlated with  $\Delta P_{\text{ETCO}_2}$  ( $r > 0.78, p < .05$ ), indicating robust and fast cerebral reactivity. However, there were profound differences in NIRS signals:

1. Under the BH task (Figure 4A), both  $\Delta[\text{HbO}]$  and  $\Delta[\text{Hb}]$  signals were highly correlated with  $\Delta\overline{BOLD}\%$  ( $\Delta[\text{HbO}]: r = 0.77 \pm 0.1, p < .005$ ;  $\Delta[\text{Hb}]: r = -0.58 \pm 0.11, p < .005$ ).

2. Under the long-ramped CI task (Figure 4B), both  $\Delta[\text{HbO}]$  and  $\Delta[\text{Hb}]$  signals were highly correlated with  $\Delta\overline{BOLD}\%$  ( $\Delta[\text{HbO}]: r = 0.68 \pm 0.06, p < 10^{-3}$ ;  $\Delta[\text{Hb}]: r = -0.62 \pm 0.15, p < .005$ ).

3. Under the short-ramped CI task (Figure 4C), relatively low MCCCs were found between NIRS signals and  $\Delta\overline{BOLD}\%$  ( $\Delta[\text{HbO}]: r = 0.49 \pm 0.29, p < .05$ ;  $\Delta[\text{Hb}]: r = -0.50 \pm 0.34, p < .05$ ). Furthermore, the standard deviations across NIRS results were large.

4. Sharp-CI task results from these four subjects were also included for ease of comparison. Under the sharp-CI task (Figure 4D), the MCCCs between NIRS signals and  $\Delta\overline{BOLD}\%$  were relatively low ( $\Delta[\text{HbO}]: r = 0.47 \pm 0.55, p < .05$ ;  $\Delta[\text{Hb}]: r = -0.32 \pm 0.45, p > .1$ ) with large standard deviations and long delays. These results are in-line with rest of the subjects discussed in section 3.1.

The averaged MCCC between  $\Delta\overline{BOLD}\%$  and NIRS signals of each channel and all tasks for the subgroup of 4 subjects was calculated (Figure 5).  $\Delta[\text{HbO}]$  and  $\Delta[\text{Hb}]$  signals were significantly correlated with  $\Delta\overline{BOLD}\%$  for most channels in the BH, long-ramped CI, and short-ramped CI task (Figure 5A-C, respectively). In contrast, Figure 5D shows that under the sharp-CI task, 47% of the  $\Delta[\text{HbO}]$  signals and 82% of the  $\Delta[\text{Hb}]$  signals were not

significantly correlated with  $\Delta\overline{BOLD}\%$ . The averaged MCCCs between the  $\Delta P_{\text{ETCO}_2}$  and NIRS signals from each channel around the prefrontal region for original sharp-CI, long-ramped CI, and short-ramped CI task are shown in the supplemental material (Figure S3).

The movies of different tasks can be found in supplemental material (Videos S1-4). Figure 6 illustrates three snapshots from one subject's long-ramped CI task movie. By mapping the spatio-temporal patterns of  $\Delta\overline{BOLD}\%$  in the brain under hypercapnia tasks, we found that brain reactions to  $\text{CO}_2$  are highly spatial-specific. As a result, NIRS signals under hypercapnia are likely to be spatial-specific as well. Moreover, it was found that the  $\Delta\overline{BOLD}\%$  from the superficial layer of the prefrontal region (black squares in Figure 6) reacted slower to  $\text{CO}_2$  when compared with the deeper layer. This observation indicated that it was incorrect to claim that NIRS signals reflect brain responses from all layers of the prefrontal cortex. Even without physiological noise from the skin and skull, NIRS may only measure responses in the superficial layer of the brain, which, based on our results, lagged the response from the deeper layer.

## 4 | DISCUSSION

The goal of this study was to better understand NIRS signals under induced-hypercapnia and establish and optimize a corresponding protocol so NIRS can be used in lieu of fMRI as an alternative, portable methodology to acquire critical brain perfusion parameters (e.g. CVR).

### 4.1 | NIRS signals under sharp-CI task

In the sharp-CI task (i.e., sharp increases in  $P_{\text{ETCO}_2}$ ), the  $\Delta\overline{BOLD}\%$ s from all subjects were highly correlated with the waveform of  $\Delta P_{\text{ETCO}_2}$ . However, NIRS reactions to the sharp increases in  $P_{\text{ETCO}_2}$  were unpredictable and highly heterogeneous both temporally and spatially. The difference between the  $\Delta\overline{BOLD}\%$  and NIRS signals relates to the fact that NIRS signals are sensitive to blood flow and volume changes in both the extracerebral and cerebral layers, while  $\Delta\overline{BOLD}\%$  reflects these changes in the cerebrum only.<sup>47, 48</sup>

Another possible explanation for difference between  $\Delta\overline{BOLD}\%$  and NIRS signals may be related to layer-specific differences in vascular reactions following exposure to sharp increases in  $P_{\text{ETCO}_2}$ . In fact, cerebrovascular responses are controlled by an autoregulation system.<sup>49</sup> A previous study found that the velocity of blood flow increased more in the cerebral circulation (about 54% increase in the internal carotid artery) than in the



extracerebral circulation (about 5% increase in the external carotid artery) under a CI task (6%  $\text{CO}_2$ ).<sup>50</sup> Similar results were also found in another study, in which greater blood flow was observed in the middle cerebral artery (cerebral) compared with the brachial artery (extracerebral).<sup>51</sup> These findings suggest that the cerebral vascular reaction is more sensitive to  $\text{P}_{\text{ETCO}_2}$  elevation than the extracerebral and peripheral vascular reactions. This makes sense, intuitively, given the criticality of brain homeostasis. In detail, blood flow would be dramatically prioritized to the brain when  $\text{P}_{\text{ETCO}_2}$  increases sharply, leading to a quick reaction observed in cerebral blood flow (observed by BOLD fMRI). In contrast, blood flow to the extracerebral layer could be dramatically compromised, leading to long delays, gradual increases, or sometimes, unpredictable changes in the extracerebral circulation (observed by NIRS).

The degree of the effect is dependent upon each individual's physiology (e.g., sensitivity to elevated  $\text{P}_{\text{ETCO}_2}$ , speed of blood flow adjustment, etc.) which could explain the highly varied NIRS results between subjects during the sharp-CI task. Based on these arguments, it is hypothesized that the cerebral and extracerebral vascular reactions could be more easily synchronized when the  $\text{P}_{\text{ETCO}_2}$  increase is not sharp, but instead slow and gradual. This gradual increase in  $\text{P}_{\text{ETCO}_2}$  would provide adequate time for the carotid artery to meet the increasing demands for both cerebral and extracerebral circulation, leading to consistent NIRS signals that would correlate better to fMRI signals.

## 4.2 | Validations

To test the hypothesis, we conducted three additional induced-hypercapnia tasks. Under the long-ramped CI task,  $\Delta\overline{\text{BOLD}}\%$  and NIRS signals correlated well and showed slow and gradual increases (decreased  $\Delta[\text{Hb}]$  signals), as suggested (Figure 4B). Furthermore, it is reasonable to assume that  $\text{P}_{\text{ETCO}_2}$  increases gradually during the BH period due to continuous and stable physiological demand and lack of air exchange. The post-exhale BH protocol used in the study<sup>36</sup> would raise  $\text{P}_{\text{ETCO}_2}$  almost immediately (compared with BH after inhalation), but slowly. If the  $\text{P}_{\text{ETCO}_2}$  increased slowly during the BH protocol, based on our hypothesis, the cerebral and extracerebral circulations should react almost simultaneously. This is exactly what was observed (Figure 4A). NIRS and  $\Delta\overline{\text{BOLD}}\%$  signals correlated well and showed gradual increases during the BH. The results are consistent with those from previous fMRI studies.<sup>21, 26, 52</sup>

Additionally, under the long-ramped CI, most of the NIRS signals had slower responses compared with the BOLD fMRI signal, which was also observed in a previous vasostimulus study (CI task).<sup>25</sup> However, the observations were different from the concurrent studies on the functional/cognitive tasks (e.g. finger tapping task, go/no go task), which showed that the NIRS ( $\Delta[\text{HbO}]$ ) reacted faster and had shorter time-to-peaks than BOLD fMRI signals.<sup>32, 53, 54</sup> The observed differences are caused by varying brain reactions to neuronal and physiological stimuli. First, the NIRS/fMRI signal from the cognitive

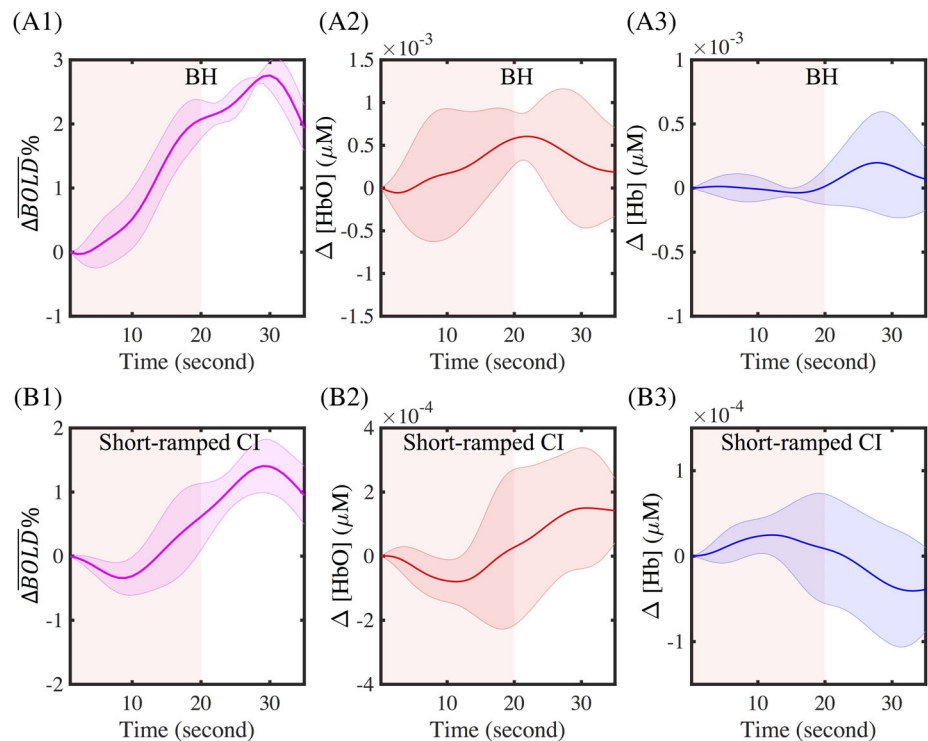


**FIGURE 7** Group folding average of signals from the A, BH and B, short-ramped CI task. The results of  $\Delta\overline{\text{BOLD}}\%$  (normalized),  $\Delta[\text{HbO}]$ , and  $\Delta[\text{Hb}]$  are showed in columns 1–3, respectively. The shaded areas (prior to 20 s) indicate the periods of BH/ramped-increased  $\text{P}_{\text{ETCO}_2}$

task results from neurovascular coupling, which is regional, while the signal in vasostimulus task results from the vasodilatory effect of CO<sub>2</sub>, which is global (including skin and skull). Second, cognitive activation is instantaneous, while elevated CO<sub>2</sub> must be carried by the blood and may reach different brain regions with varying time delays. Third, different brain regions react differently to arriving CO<sub>2</sub> based on the local hemodynamic response function, which can lead to further delays. In Figure 6, we observed that the  $\Delta\overline{BOLD}\%$  response to CO<sub>2</sub> was significantly lagged at the superficial layer of the prefrontal cortex when compared with deeper cortical layers. Since the NIRS probe was placed over the prefrontal area, the lagged signal could be captured by the NIRS probe, thus resulting in observed delays.

Finally, the short-ramped CI task was introduced to simulate the BH task (validating the gradual increase of P<sub>ET</sub>CO<sub>2</sub> during the BH). The NIRS signal ( $\Delta[\text{HbO}]$ , Figure 4C) was expected to be similar to the signal obtained from the BH task (Figure 4A). The results demonstrated that the NIRS signal does change according to the task (Figure 4C), albeit with much more noise than that of BH task-related signals (Figure 4A). The main reason could be that subjects had to physically breathe in order to reach the P<sub>ET</sub>CO<sub>2</sub> level during the short-ramped CI task, while during the BH, no breathing was required. As result, NIRS signals in the short-ramped CI task may have been influenced by the side effects of respiration, such as motion and other related physiological processes. To remove the noise, a folding average of the NIRS signals (Figure 7) was calculated. The averaged NIRS epoch signals from the short-ramped CI task (Figure 7A) and BH (Figure 7B) were similar, and both were highly correlated with averaged  $\Delta\overline{BOLD}\%$  signals. The delay observed in the data from the short-ramped CI task may have been due to the time lag for the inhaled CO<sub>2</sub> to reach the brain.

### 4.3 | Limitations

This study provides possible physiological explanations for the discrepancies observed between BH- and CI-related NIRS signals; however, several limitations exist. First, the source-detector distance was about 3 cm, which is commonly used in NIRS studies.<sup>23, 24</sup> However, other studies used longer source-detector distances ( $\geq 4$  cm), and were therefore less prone to signals from the extracerebral layers. Consequently, these studies demonstrated more robust and consistent NIRS results.<sup>20, 23, 25</sup> Second, during the BH period, it was difficult to assess P<sub>ET</sub>CO<sub>2</sub> changes (i.e. there was no exhaled breath to measure). Third, the NIRS probe was placed over the prefrontal region, which is a popular region of interest since

there is little-to-no hair. However, this study found that hemodynamic responses under hypercapnia tasks are highly spatial-specific. Thus, whole brain measurements using NIRS channels may be required to capture region-specific reactions to hypercapnia tasks. Finally, future studies should incorporate measuring P<sub>ET</sub>CO<sub>2</sub> changes that occur during the BH task. For example, previous studies required subjects to perform a forced exhalation at the end of each BH period – this could be incorporated in future studies.<sup>38, 52</sup>

## 5 | CONCLUSION

In summary, the presented study, together with previous studies, support the hypothesis that cerebral and extracerebral reactivity to elevated P<sub>ET</sub>CO<sub>2</sub> are similar when the increase of P<sub>ET</sub>CO<sub>2</sub> is gradual, and are different when the increase of P<sub>ET</sub>CO<sub>2</sub> is sharp. Further, it demonstrated that NIRS can be deployed as an alternative low-cost, real-time, and non-invasive methodology for reliably measuring the cerebrovascular reaction given the correct vasoactive stress tests (e.g. long-ramped CI and BH task). This would benefit a large population who require timely (e.g. athletes) and/or on-site (e.g. infants or patients with immobility) measurements of cerebral reactivity.

## ACKNOWLEDGMENTS

This work was supported by the National Institutes of Health, Grants K25 DA031769 (YT); in part, with support from the Indiana Clinical and Translational Sciences Institute (the Pilot Funding for Research Use of Core Facilities). One author (Taylor Lee) was supported by National Science Foundation Graduate Research Fellowship under Grant No. DGE-1333468.

## CONFLICT OF INTEREST

The authors have no conflict of interest.

## ORCID

Ho-Ching (Shawn) Yang  <https://orcid.org/0000-0003-2670-1772>

## REFERENCES

- [1] T. L. Davis, K. K. Kwong, R. M. Weisskoff, B. R. Rosen, *Proc. Natl. Acad. Sci. U. S. A.* **1998**, 95, 1834.
- [2] R. D. Hoge, J. Atkinson, B. Gill, G. R. Crelmer, S. Marrett, G. B. Pike, *Magn. Reson. Med.* **1999**, 42, 849.
- [3] P. A. Chiarelli, D. P. Bulte, D. Gallichan, S. K. Piechnik, R. Wise, P. Jeppard, *J. Int. Soc. Magn. Reson. Med.* **2007**, 57, 538.
- [4] F. M. Faraci, K. R. Breese, D. D. Heistad, *Stroke* **1994**, 25, 1679.
- [5] S. H. Yoon, M. Zuccarello, R. M. Rapoport General, *Pharmacol.: The Vasc. Syst.* **2000**, 35, 333.

- [6] N. A. Lassen, *Taylor & Francis* **1968**, 22, 247.
- [7] B. Stefanovic, J. M. Warnking, E. Kobayashi, A. P. Bagshaw, C. Hawco, F. Dubeau, J. Gotman, G. B. Pike, *Neuroimage* **2005**, 28, 205.
- [8] C. W. Barten, E. S. Wang, *Ann. Emerg. Med.* **1994**, 23, 560.
- [9] E. Prisman, M. Slessarev, J. Han, J. Poublanc, A. Mardimae, A. Crawley, J. Fisher, D. Mikulis, *J. Int. Soc. Magn. Reson. Med.* **2008**, 27, 185.
- [10] E. Rostrup, H. B. Larsson, P. B. Toft, K. Garde, C. Thomsen, P. Ring, L. Søndergaard, O. Henriksen, *NMR Biomed.* **1994**, 7, 29.
- [11] U. S. Yezhuvath, K. Lewis-Amezcu, R. Varghese, G. Xiao, H. Lu, *NMR Biomed.* **2009**, 22, 779.
- [12] R. G. Wise, K. T. Pattinson, D. P. Bulte, P. A. Chiarelli, S. D. Mayhew, G. M. Balanos, D. F. O'Connor, T. R. Pragnell, P. A. Robbins, I. Tracey, *Journal of Cerebral Blood Flow & Metabolism.* **2007**, 27, 1521.
- [13] M. Slessarev, J. Han, A. Mardimae, E. Prisman, D. Preiss, G. Volgyesi, C. Ansel, J. Duffin, J. A. Fisher, *J. Physiol.* **2007**, 581, 1207.
- [14] A. Kastrup, T.-Q. Li, A. Takahashi, G. H. Glover, M. E. Moseley, *Stroke* **1998**, 29, 2641.
- [15] H. Markus, M. Harrison, *Stroke* **1992**, 23, 668.
- [16] D. A. Boas, C. E. Elwell, M. Ferrari, G. Taga, *Neuroimage* **2014**, 85, 1.
- [17] M. Ferrari, V. Quaresima, *Neuroimage* **2012**, 63, 921.
- [18] F. Scholkmann, S. Kleiser, A. J. Metz, R. Zimmermann, J. M. Pavia, U. Wolf, M. Wolf, *Neuroimage* **2014**, 85, 6.
- [19] M. Wolf, M. Ferrari, V. Quaresima, *J. Biomed. Opt.* **2007**, 12, 062104.
- [20] P. Smielewski, P. Kirkpatrick, P. Minhas, J. D. Pickard, M. Czosnyka, *Stroke* **1995**, 26, 2285.
- [21] U. Emir, C. Ozturk, A. Akin, *Physiol. Meas.* **2007**, 29, 49.
- [22] T. S. Leung, I. Tachtsidis, M. M. Tisdall, C. Pritchard, M. Smith, C. E. Elwell, *Physiol. Meas.* **2008**, 30, 1.
- [23] J. Virtanen, T. E. Noponen, P. Meriläinen, *J. Biomed. Opt.* **2009**, 14, 054032.
- [24] J. J. Selb, D. A. Boas, S.-T. Chan, K. C. Evans, E. M. Buckley, S. A. Carp, *Neurophotonics.* **2014**, 1, 015005.
- [25] T. Alderliesten, J. De Vis, P. Lemmers, F. Van Bel, M. Benders, J. Hendrikse, E. Petersen, *Neuroimage* **2014**, 85, 255.
- [26] B. J. MacIntosh, L. M. Klassen, R. S. Menon, *Neuroimage* **2003**, 20, 1246.
- [27] D. O. Svaldi, C. Joshi, M. E. Robinson, T. E. Shenk, K. Abbas, E. A. Nauman, L. J. Leverenz, T. M. Talavage, *Dev. Neuropsychol.* **2015**, 40, 80.
- [28] D. O. Svaldi, E. C. McCuen, C. Joshi, M. E. Robinson, Y. Nho, R. Hannemann, E. A. Nauman, L. J. Leverenz, T. M. Talavage, *Brain Imaging Behav.* **2017**, 11, 98.
- [29] D. O. Svaldi, C. Joshi, E. C. McCuen, J. P. Music, R. Hannemann, L. J. Leverenz, E. A. Nauman, T. M. Talavage, *Brain Imaging Behav.* **2018**, 14, 164.
- [30] A. Riecker, W. Grodd, U. Klose, J. B. Schulz, K. Gröschel, M. Erb, H. Ackermann, A. Kastrup, *J. Cereb. Blood Flow Metab.* **2003**, 23, 565.
- [31] J. F. Schieve, W. P. Wilson, *Am. J. Med.* **1953**, 15, 171.
- [32] L. Gagnon, M. A. Yücel, M. Dehaes, R. J. Cooper, K. L. Perdue, J. Selb, T. J. Huppert, R. D. Hoge, D. A. Boas, *Neuroimage* **2012**, 59, 3933.
- [33] T. Funane, H. Atsumori, T. Katura, A. N. Obata, H. Sato, Y. Tanikawa, E. Okada, M. Kiguchi, *Neuroimage* **2014**, 85, 150.
- [34] D. Harris, F. Cowans, D. Wertheim, In *Oxygen Transport to tissue XV*, Springer, Boston, MA, **1994**, pp. 825.
- [35] J. Duffin, O. Sobczyk, A. Crawley, J. Poublanc, L. Venkatraghavan, K. Sam, A. Mutch, D. Mikulis, J. Fisher, *Hum. Brain Mapp.* **2017**, 38, 5590.
- [36] M. G. Bright, K. Murphy, *Neuroimage* **2013**, 83, 559.
- [37] J. Peirce, J. R. Gray, S. Simpson, M. MacAskill, R. Höchenberger, H. Sogo, E. Kastman, J. K. Lindeløv, *Behav. Res. Methods* **2019**, 51, 195.
- [38] F. B. Tancredi, *J. Cereb. Blood Flow Metab.* **2013**, 33, 1066.
- [39] Y. Xu, H. L. Graber, R. L. Barbour, nirsLAB: a computing environment for fNIRS neuroimaging data analysis. In: *Biomedical Optics*, Miami, FL, April, **2014**, pp. BM3A.1.
- [40] G. Strangman, J. P. Culver, J. H. Thompson, D. A. Boas, *Neuroimage* **2002**, 17, 719.
- [41] M. Jenkinson, C. F. Beckmann, T. E. Behrens, M. W. Woolrich, S. M. Smith, *Neuroimage* **2012**, 62, 782.
- [42] J. D. Power, A. Mitra, T. O. Laumann, A. Z. Snyder, B. L. Schlaggar, S. E. Petersen, *Neuroimage* **2014**, 84, 320.
- [43] X. Shen, F. Tokoglu, X. Papademetris, R. T. Constable, *Neuroimage* **2013**, 82, 403.
- [44] R. A. Fisher, *Biometrika* **1915**, 10, 507.
- [45] R. A. Fisher, *Metron.* **1921**, 1, 1.
- [46] C. R. Genovese, N. A. Lazar, T. Nichols, *Neuroimage* **2002**, 15, 870.
- [47] P. W. McCormick, M. Stewart, G. Lewis, M. Dujovny, J. I. Ausman, *J. Neurosurg.* **1992**, 76, 315.
- [48] R. B. Saager, A. J. Berger, *JOSA A* **2005**, 22, 1874.
- [49] O. Paulson, S. Strandgaard, L. Edvinsson, *Cerebrovasc. Brain Metab. Rev.* **1990**, 2, 161.
- [50] K. Sato, T. Sadamoto, A. Hirasawa, A. Oue, A. W. Subudhi, T. Miyazawa, S. Ogoh, *J. Phys. I* **2012**, 590, 3277.
- [51] J. S. Vantanajal, J. C. Ashmead, T. J. Anderson, R. T. Hepple, M. J. Poulin, *J. Appl. Physiol.* **2007**, 102, 87.
- [52] K. Murphy, A. D. Harris, R. G. Wise, *Neuroimage* **2011**, 54, 369.
- [53] T. J. Huppert, R. D. Hoge, S. G. Diamond, M. A. Franceschini, D. A. Boas, *Neuroimage* **2006**, 29, 368.
- [54] D. A. Boas, T. Gaudette, G. Strangman, X. Cheng, J. J. Marota, J. B. Mandeville, *Neuroimage* **2001**, 13, 76.

## SUPPORTING INFORMATION

Additional supporting information may be found online in the Supporting Information section at the end of this article.

**How to cite this article:** Yang H-C, Liang Z, Vike NL, et al. Characterizing near-infrared spectroscopy signal under hypercapnia. *J. Biophotonics*. 2020;e202000173. <https://doi.org/10.1002/jbio.202000173>